Evaluation of Soil Liquefaction Potential by Sensitivity Analysis, Reliability and Data validation

Mohammad Alizadeh Mansouri[1], Rouzbeh Dabiri[2*]

1. Department of Civil Engineering, Sofian Branch, Islamic Azad University, Sofian, Iran.

2. Department of Civil Engineering, Tabriz Branch, Islamic Azad University, Tabriz, Iran

Received: 2021/2/18 Accepted: 2021/3/10

ABSTRACT

In this study, it is attempted to analyze sensitivity and reliability in order to evaluate the liquefaction potential in soil layers in Tabriz. 62 boreholes that had possible conditions for liquefaction were selected. Seismic mapping was simulated using finite fault method and then the effect of soil layers on PGA was estimated. In continue, the liquefaction potential index was estimated and the zoning map of liquefaction risk was presented. In final, through sensitivity and reliability analysis of the Monte Carlo method, the rate of density function against safety factor of the soil layers versus to liquefaction was determined.

Keywords: Liquefaction, Sensitivity Analysis, Reliability, Monte Carlo Method, Data validation, Tabriz.

1. INTRODUCTION

One of the major seismic geotechnical events causing severe damage during an earthquake is the phenomenon of liquefaction. Due to increase in the water pressure of the void in the loose soil layers (in a special case) because of the vibrations caused by the earthquake and the tendency to contract the volume, a reduction of confining stress in the soil occurs in which shear strength behavior is severely concentrated almost to zero. This condition is called liquefaction. This phenomenon manifests itself in the form of extensive settlement, sand,

*Corresponding author: rouzbeh_dabiri@iaut.ac.ir

mud and water boils, and water leakage from pores on the ground's surface. Various factors can affect the occurrence of liquefaction in soil layers, which can be attributed to the earthquake magnitude and its duration, porosity or void ratio, relative density, fine percentage and plastic limit and the range of shear stress applied to the soil mass. The main purpose of this study is to evaluate the potential of soil liquefaction in Tabriz city based on sensitivity and reliability analysis with control data and testing approach (verification) that utilizes peak ground acceleration caused by North Tabriz fault estimated by limited seismic simulation, which will be described in the following.

2. LIQUEFACTION AND PEAK GROUND ACCELARATION

If a saturated sand deposit vibrates, it tends to decrease in volume. In case drainage is not available, the result will be an increase in pore pressure. If the water pressure in the sand deposits increases due to continuous vibration, sometimes the amount may be equal to the total stress. Based on the concept of effective stress, it can be written:

$$\sigma' = \sigma - u \quad (1)$$

In the above relation, σ', σ, and u are respectively the effective stress, total stress and pore water pressure. In case the total stress is equal to the pore water pressure, then the effective stress is equal to zero. In this condition, the sand will not have any shear strength and will become liquid. This state is called liquefaction. Liquefaction of saturated sand during earthquakes has been the cause of extensive damage and destruction to buildings, dams, and retaining structures [1]. In recent years, various laboratory and field methods have been proposed to evaluate the liquefaction resistance of soils. Field methods include standard penetration tests [2, 3] cone penetration resistance [4] and geophysical experiments with shear wave velocity measurements [5,6]. Regarding evaluation of the potential of liquefaction in the city of Tabriz, we can mention the studies conducted by Ghasemian et al. [7] and Oshnoyeh and Dabiri [8].

On the other hand, as mentioned above, one of the important and effective parameters in estimating the potential of liquefaction in soil stratifications is the peak ground acceleration (PGA). Extensive studies have been conducted to estimate the PGA in the Iranian plateau [9-

12]. Considering that the study area is the city of Tabriz and the fault of the north of Tabriz is one of the faults in region, as a result, accurate evaluation of the PGA is significant. In the present study, a randomized finite fault method was utilized to predict the strong movements of the ground. The limited fault source model is a significant tool for estimating movements near the epicenter. In modeling a strong earthquake, when the site is far enough away from the source of the earthquake (fault), the source of the earthquake can be assumed to be a point source; however, in the near field, cases such as fault geometry, heterogeneous distribution of earthquake on the fault surface and direction can have great impact on the content of the resulting movement [13].

3. SENSITIVITY AND RELIABILITY ANALYSIS

3.1. Sensitivity Analysis

Sensitivity analysis is the study of the effectiveness of input variables on output variables of a statistical model. In other words, it is a method of changing the inputs of an organized (systematic) statistical model that can predict the effects of these changes on the output of the model. In fact, sensitivity analysis determines, considering a set of specific hypotheses, how a different value of an independent variable such as x_1, x_2, x_3, …, x_n affects a dependent variable such as y. This technique is used by applying certain boundary conditions, which rely on one or more input variables. Sensitivity analysis methods can be categorized into three groups: mathematical, statistical (probabilistic) and graphical. This classification helps determine the ability of each of the sensitivity analysis methods for different models and to select the appropriate methods according to the characteristics of each for decision making. Mathematical methods are suitable for definite and probabilistic models, statistical methods are normally applied to probabilistic models and models derived from random data and variables, and graphical methods are typically utilized for both mathematical and statistical models. Pattern identification and classification is one of the most main applications of statistical methods in various fields. One of the main goals of modeling and classification in statistics is estimation based on existing facts and variables and available information on a specific topic. It is achieved in statistical studies mainly by methods such as regression, audit analysis, time series, classification, tree regression and other statistical methods. The

Multiple Linear Regression (MLR) method describes the relationship between a series of predictive variables and the desired response variable. If there are independent variables x1, x2, x3, …, xn, in order to establish their linear relationship with the dependent variable Y, the following function must be created:

$$y = f(x_1, x_2, x_3, \dots, x_n) \text{ or } \quad y = \beta_0+\beta_1x_1+\beta_2x_2+ \dots +\beta_nx_n+e \qquad (2)$$

In this regard, β1, β2, …, βn are referred to as regression coefficients and e is the value of computational error. These coefficients are indefinite, which are the estimators of the response parameter. Therefore, it is possible to analyze several different variables simultaneously, yet, to get the desired results through MLR, the number of samples must be large and accurate; therefore, this method is highly sensitive and may lead to errors in the results. In addition, in order to apply this method, variables must have a normal distribution and their changes must follow a linear relationship. Hence, there is a need for methods that have fewer limitations in this area. Meanwhile, the Artificial Neural Networks (ANN) can be also one of the most appropriate methods. Given that the neural network does not impose any initial assumptions on the distribution of data, it does not execute any constraints on the form of the function and also the relationship between the independent and dependent variables, since it is the neural network that ascertains the relation of the function itself, which is not essentially a linear relationship. Another advantage of an artificial neural network is that the information is processed implicitly. Accordingly, if part of the network cells is uninvolved or malfunctioned, there is still the possibility of reaching the correct answer; moreover, the generalizability of the neural network allows the model in connection to untrained observance to provide an appropriate answer. Thus, the application of sensitivity analysis based on neural network (ANN) has more adequate results than regression probabilistic models in determining the sensitive parameters that is significant in characterizing the dependent variables. An artificial neural network consists of a set of interconnected neurons, each of which is called a layer. The role of neurons in neural networks is to process information. It is achieved in artificial neural networks by a mathematical processor, which is the very activator function. This function is selected by the designer concerning the specific need of the problem to be solved by the neural network. The simplest form of this network is

a network that has two layers (input and output layers). The network acts like an input and output system and utilizes the value of the input neurons to calculate the value of the output neuron. Neural networks with hidden layers have more capabilities than double-layer neural networks. Multi-Layer Perceptron (MLP) works in such a way that a pattern is provided to the network and its output is calculated. Comparing the actual output and the desired output causes the network weight factor to change so that a more accurate output is obtained the next time. Depending on the purpose of the research, different types of neural networks can be applied.

3.2. Reliability Analysis

Reliability is one of the main qualitative characteristics in designing and analyzing large and complex systems, which has a significant role and importance in evaluating objectives and examining their current situation. All reliability relationships are centered on probabilistic theories. Typically the parameters in this space are measured as a random variable. In probabilistic space, each variable is characterized by a general characteristic called the probability density distribution function of that variable. Based on these functions, the variables are defined by the two characteristics of the mean value and the standard deviation in the probability density distribution function. This method, by fashioning a logical solution, determines the safety factor in proportion to the degree of unreliability of the parameters and the degree of standard risk. Reliability analysis can be applied as an alternative or supplement to definitive methods and makes it easier to judge engineering. Evaluation of the liquefaction potential normally implicates a set of definite and probabilistic methods. Definite methods, despite their simplicity, are incapable of considering unreliability. Given the soil conditions and the seismic load of an accidental nature, the definitive analysis of this phenomenon does not seem to be accurate enough so that the reliability analysis is one of the most appropriate ways to reflect on unreliability. These methods are able to quantify the degree of unreliability in the design due to the significance of the structure. This concept is usually used to express the degree of assurance of the correct operation of a part or in general a set of factors over a specified period of time and in duration. In other words, reliability theory is in fact a new way to express the accuracy and

functionality of a system against the factors affecting it. In general, reliability analysis methods are classified into three categories: analytical methods, approximate methods and simulation methods. In analytical methods, the probability function of the input parameters is expressed mathematically and then the safety factor is determined based on the aggregation on the probability values of the input parameters. Due to the fact that the criterion for calculating the exact mathematical relations is the analysis process, it is very complex so that less applicable. In approximate methods, reliability is studied concerning important probabilistic characteristics (such as mean, standard deviation and change coefficient), which are generally divided into two types of regional estimation (FOSM, FORM, AFORM) and point estimation (PEM). Approximate methods, despite estimating mean values, standard deviation, and reliability, cannot express the density function of probability and are less accurate. However, simulation-oriented methods with input parameters as random variables and repetition in calculations can analyze reliability with adequate accuracy. Of course, using this method requires intelligent calculations. The Monte Carlo Simulation method is one of the most widely used of these methods. In the Monte Carlo method, any process of a random nature is a statistical process. Since the occurrence of malfunctions in the functional mechanisms of technical engineering systems and its components is a random phenomenon, the probability of optimal function of a system in predetermined conditions and for a certain period of time is called reliability. One powerful tool for studying reliability is Monte Carlo simulation. The Monte Carlo method can be applied to estimate the probability of failure based on three basic steps as follows:

1-Random production of numbers using the cumulative distribution function of the probability of random variables in the range of zero and one ($Xi\epsilon$ [0.1])

2- Estimation of the value of each random variable using the statistical characteristics of random variables based on the randomly produced number in step one.

3- Estimation of the function of limit conditions according to the produced data of the second step and estimating the probability of failure

This method is a simple random sampling based on producing sequences of random samples in which each random variable Xi is randomly sampled and then the limit state function is

examined. If there is g (Xi) <0, then the produced random sample of Xi data will be in the failing zone, otherwise in the health zone. This test requires continuous repetitions, in each of which the Xi random variable is randomly selected to produce several points in the failing zone. Finally, for the N test, the approximate probability of failure is equal to (3).

$$P_f = \frac{n(g \leq 0)}{N} \tag{3}$$

In which, n (g≤0) is the number of tests in which g≤0 and N are the total number of tests. Obviously, the accuracy of the P_f value depends entirely on the number of repetitions of the test. As there are no limitations in the type and shape of the function and the type of variables, this method can be applied to various fields of science. The number of repetitions of the test can be determined from the relation provided by Phoon [14].

$$N = \left[\frac{Z^2}{4(1-r)}\right]^m \tag{4}$$

In this case, Z is the cumulative probability, r is the reliable level, and m is the number of variables affected. To produce random variables, functions are often applied that can put the numbers X1, X2,…, Xn in the numerical range [0,1]. With the help of the central limit theorem, it can be indicated that the sum of a large number of independent random variables has a normal or Gaussian distribution. To produce random numbers with a normal distribution in the range (-∞, + ∞), first two random numbers X1, X2 are produced in the numerical range [0,1], and then by placing in the following relations, the random variables Y1, Y2 that have a normal distribution are created.

$$\begin{cases} Y_1 = \sqrt{-2L_n(X_1)}\, Cos(2\pi X_2) \\ Y_2 = \sqrt{-2L_n(X_1)}\, Sin(2\pi X_2) \end{cases} \tag{5}$$

The following equations (4) and (5) are used to estimate the reliability of R (t) and the failure rate λ (t) at each stage of the simulation using random numbers produced by the normal distribution.

$$R(t) = \int_t^{+\infty} f(u)d_u = \int_t^{+\infty} \frac{1}{\sigma\sqrt{2\pi}} e^{\frac{1}{2}\left[\frac{u-\mu}{\sigma}\right]^2} d_t \tag{6}$$

$$\lambda(t) = -\frac{Ln(1-\varphi\left(\frac{t-\mu}{\sigma}\right))}{t} \tag{7}$$

In this regard, several researchers such as Idriss and Boulanger [2], Juang et al. [15], Idriss and Boulanger [16], Johari and khodaparast [17], Janalizade et al. [18], Pirhadi et al. [19] have been applied different methods. However, among them, the researches by Juang et al. [15] and Idriss and Boulanger [16] are of great significance. Based on this reliability research, they have been able to establish a mathematical and logical relationship for announcing changes in the probability of liquefaction with a safety factor, which are presented in equations No.8 and No.9, respectively.

$$PL = 1 - \emptyset\left[\frac{L_n(F.S)+0.13}{0.13}\right], \text{ Boulanger and Idriss (2014)} \quad (8)$$

$$PL = \frac{1}{1+\exp[7.545(F.S-0.952)]}, \text{ Juang et al. (2012)} \quad (9)$$

In the following, first the geological conditions in the study area are presented and then the evaluation of peak ground acceleration, and finally, the evaluation of liquefaction potential based on sensitivity and reliability analysis methods are discussed.

4. GENERAL CONDITIONS AND SOIL STRATIFICATION

The city of Tabriz is surrounded by the Eynali (Oon-Ebne-Ali) mountain range in the east-west, and not-so-high consolidated alluvial deposits and conglomerates in the south. The general slope of the plain is towards the west and, as a result, the direction of the general drainage of the surface and underground water is also westward. The surface of the plain is generally covered by alluvial deposits. The average height of the city of Tabriz is 1340 metres above sea level (Figure 1).

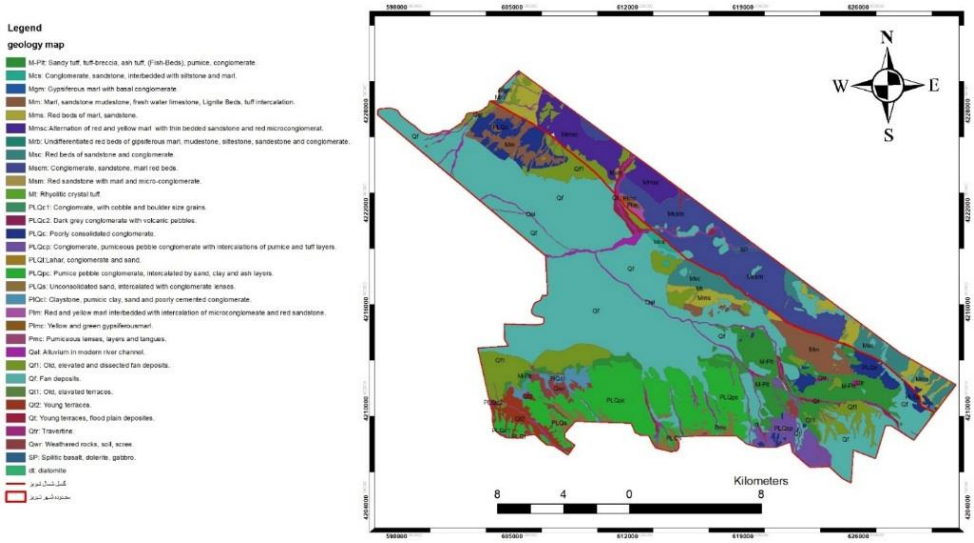

Figure1. Geological Map of Tabriz.

4.1. Soil Stratification in study area

Azerbaijan, with respect to stratigraphy, has a long period of expansion and the surroundings of the Tabriz plain also have extensive Cambrian outcrops, but the stones and the alluvium in the area of Tabriz do not date back to such a time period with their formation components being related to the Cenozoic and Quaternary periods. The Cainozoic component in the Tabriz plain started from the Miocene Age and lasted up to the Quaternary era. There is no indication of Palaeocene, Eocene and Oligocene- sediments to indicate pre-Miocene formations, proving that the area is not stratigraphic in nature. The area under study is inside the city of Tabriz, in the southern part of the mountain range of Eynali that passes through the red Continental classic sediments (mid Miocene) and young alluvial sediment. The red sediments have gypsum and salt. This formation is mostly composed of sand stone, marl, siltstone and conglomerates along with gypsum and salt. In this area of Tabriz, the continental sediments of Pons have traces of coal. The mentioned coal is not pure and has been found to be in the form of short and inapplicable shape existing in the hills of Baghmishe and Sari Dagh inside the yellow and fossiliferous marl. The marly-hilly formation of Baghmishe that contains coal in the south-west of Tabriz has an outcrop of high thickness, and fish sediment has been located on them at Sinitic, Lapilli and Diatomite. The alluvial of the fourth period including soft to hard conglomerates is located on this sediment. Under the alucia depostes of the Abbasi street towards the east, there are marn and sandstone

conglomerate layers at a dept of less than 10 metres. The geological sequances and formations of Tabriz are shown in Table 1 [7].

Table 1: Geological Sequances and formations of Tabriz [7].

Quaternary	Alluvium
Pliocene	Fish beds (marl, lapilli, diatomite)
Miocene	Baghmishe formation (marl with shale and lignite) Upper red formation (marl, sandstone, claystone with layer of gypsum)

4.2. Structural Geology

The city of Tabriz is located in the west Alborz zone and follows the tectonic regimes ruling it. The forming of the Tabriz plain sediment in it and the formation of tectonic structures that often emerge as fractures or faults follow this system. The Tabriz plain is surrounded in the north by the mountains of Eynali and on the south by the volcanic altitudes of Sahand and its pyroclastic sediments. The reverse function of the north Tabriz Fault with the slope to the north had caused the collapse of its southern part. As a result, parallel to the northern part fractures with normal displacement, the southern plains have been created, resulting in a gardenlike collapse of the east-west continuation. The current formation on which Tabriz is located is the result of such a collapse. As a result of this collapse, the rest of the Miocene and pyroclastic sediment of the east and the south of the city are observable in lower height balances. Furthermore, the erosive function due to the entrance of the big rivers caused the deposit of alluvial material with high thickness in the plain. Regarding the headwaters of the river from the south and the east of the Tabriz plain and its elongation in an east-west state by moving towards the west, particle reduction is expected. According to the fault system activity and the occurred earthquakes in the region and observation of fractures in younger sediments, the area is tectonically active. The Alpine-Himalayan belt is one of the world's most important seismic belts, in which Iran is located. Azerbaijan is also located in this belt and had experienced destructive earthquakes in the past. There are many large and small faults in the region that may cause destructive tremors.

5. EVALUATION OF THE LIQUEFACTION POTENTIAL IN THE STUDY AREA

In order to evaluate the liquefaction potential of soil stratifications in the city of Tabriz, geotechnical data of 446 boreholes were evaluated. 260 boreholes had complete geotechnical data and 62 boreholes, regarding reliability analysis, were selected in the area of city of Tabriz concerning geotechnical characteristics with probability of liquefaction (Figure 2). Groundwater levels are one of the main factors in assessing the potential for soil liquefaction. The amount of changes in the city of Tabriz can be observed according to the reports of the Regional Water Organization of East Azerbaijan Province and based on the groundwater level in the piezometers and the borehole log according to Figure 3.

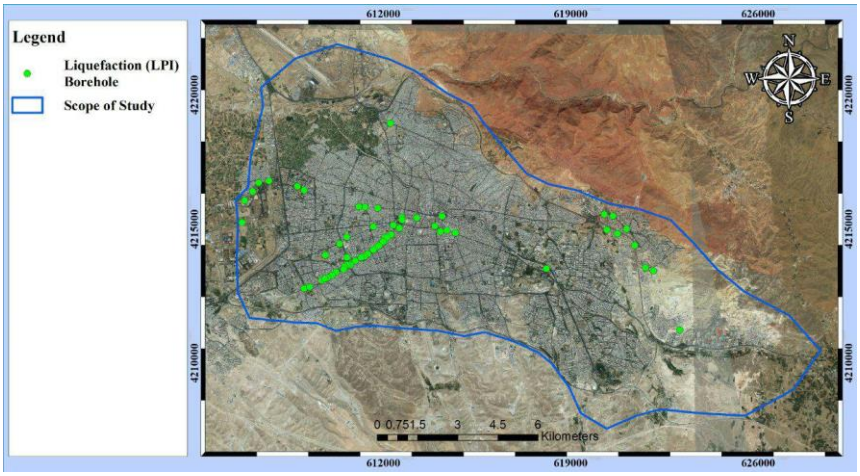

Figure2. Location of boreholes that have liquefaction potential in study area.

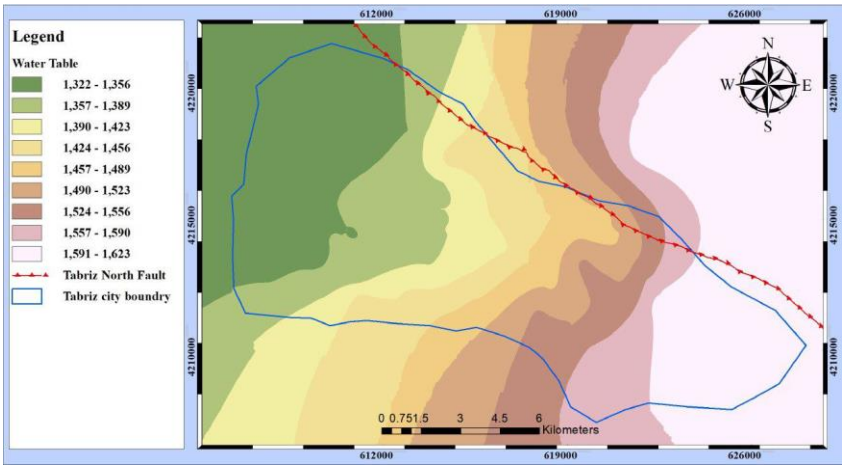

Figure3. Variations of ground water level in study area.

5.1. Determining the Maximum Surface Acceleration

The area of Tabriz city is located in the northwest of Iran and near one of the important and recognized seismic faults of the Iranian plateau (North Tabriz Fault). The North Tabriz Fault is considered to be seismic and active fault with the occurrence of at least 16 historical earthquakes [20]. Studies indicate that this fault has a length of about 150 km and its rupture can be very dangerous due to the fact that it is located within the urban area of Tabriz. Figure 4 shows the faults in the area; as it can be seen, the North Tabriz Fault is the longest active fault that a significant part of which is located within the urban area.

According to the mentioned cases and the significance of issue in this research, seismic zoning of Tabriz city has been reflected due to the activation of the North Tabriz Fault. To this end, a limited random fault method has been applied to predict the strong movement of the earth. The limited fault source model is an important tool for predicting ground movements near the epicenter. In modeling a strong earthquake, when the site is far enough away from the source of the earthquake (fault), the source of the earthquake can be assumed to be a point source; however, in the near field, cases such as fault geometry, heterogeneous distribution of slip on the fault surface and direction can have a great impact on the content of the resulting movement [13]. In order to evaluate these effects of limited fault in ground movement modeling, Hartzel [21] proposed to divide the fault level of an earthquake into network of sub-sources, each of which can be considered as a point source [22]. A fault surface, a certain size, is divided into an array of sub-sources, each of which behaves as a point source, depending on the moment of the earthquake. The time series subset of the series model utilizes a random point source developed by Boore [23] using a random method simulated with a generalized computer code [24]. In recent years, researchers have studied to obtain the maximum strong ground movement using a randomized finite fault method, which the researches by Samaei et al. [25], and Amiranlu et al. [26] can be mentioned in this regard. In this study, by selecting the appropriate parameters and using the random limited fault method, the maximum horizontal acceleration due to activation of Tabriz fault, which is required to evaluate the liquefaction potential in soil stratifications, has been calculated.

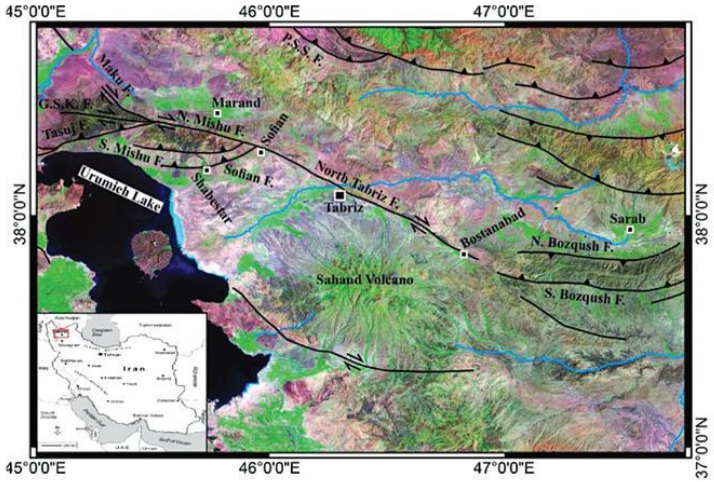

Figure 4. Map of active faults in northwest of Iran plateau.

In this study, the EXSIM program, an open-source randomized simulation algorithm written in FORTRAN, was applied to create a time series of movements for the earthquake. In limited fault modeling of seismic movement, a large fault is divided into N sub-faults, where each fault is considered as a small point source. Ground movements made by each sub-fault can be calculated by a random point method, and, after being collected at the observation point, can be obtained with a suitable time delay for the ground movement resulting from the whole fault. In this study, the fault length is about 150 km and its width is 12 km, its slope angle is 87° and based on the recorded earthquake in the region, the seismic depth is estimated from 10 to 20 km, which is in the category of surface earthquakes [27-28]. The key input parameters for simulating the acceleration of artificial mapping by random fault method and with the help of EXSIM program for North Tabriz Fault are presented in Table 2. After selecting the appropriate parameters for modeling, the simulation was carried out concerning the mentioned parameters on the seismic bed rock surface. Figure 5 indicates the points where the strong movement is simulated. By obtaining the results of the acceleration maps and drawing them based on the acceleration and distance, the maximum ground acceleration (PGA) is obtained from the sum of the answers. In Figure 6, the map of concave lines for maximum simulated horizontal acceleration is presented.

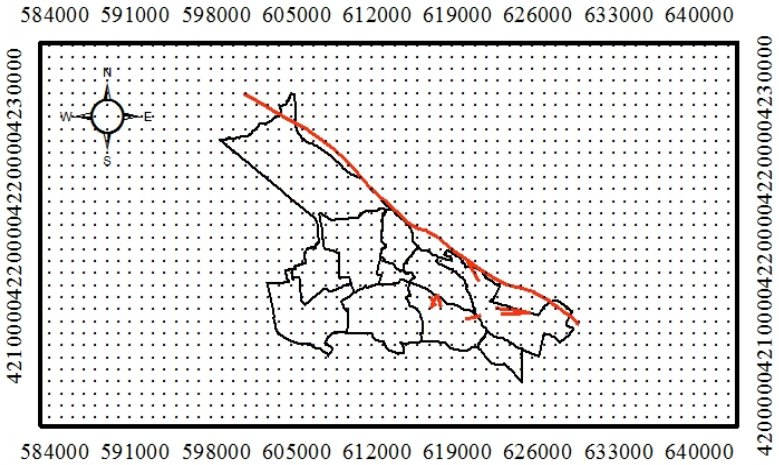

Figure 5. Points where artificial acceleration was produced.

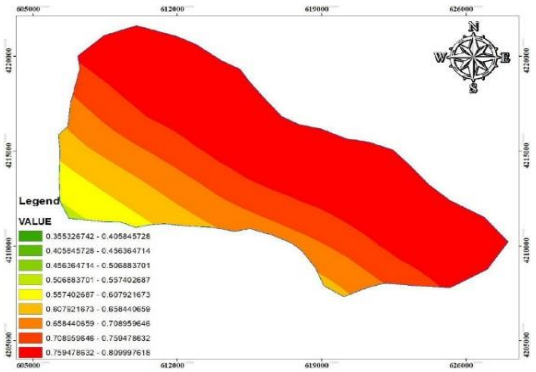

Figure 6. The simulated horizontal maximum acceleration map in study area.

Table 2: Input parameters for modeling.

EXSIM input parameters	value
The extension of fault	310°
The slope of the fault	87°
Upper depth of fault plate (km)	5
Dimensions below faults (km)	2 × 2
Largeness of torque	7.5
Tension drop (bar)	60
Geometric distribution	$\frac{1}{R}, R \leq 85\ km$ $\frac{1}{R^0}, 85 < R < 120\ km$ $\frac{1}{R^{0.5}}, R \geq 120\ km$

Quality factor Q (f)	$95f^{0.8}$
Durability	$T_0 + 0.1R$
Kappa coefficient	0.03
Beating level	50%
Subjective function	Saragoni-Hart
Shear wave velocity (km / s)	3.3
Velocity of dispersion	0.8 × Shear wave velocity
Shell density (g / cm^3)	2.8
Damping	5%
The element from which the rupture begins	Random
Seismic distribution	Random

As it is observed, the maximum horizontal acceleration produced by the North Tabriz Fault in the northern parts of the city reaches 0.80 g, while the maximum acceleration in the southern parts is reduced to 0.04g. Due to the risk of direct rupture in the city, faults in the city of Tabriz and the effects of the area near the fault in the event of an earthquake may cause many casualties and damages in Tabriz. In settlements such as Baghmisheh, Rushdieh, the northern parts of Tabriz, and the area near the fault, due to the existence of marl-clay deposits, the potential for landslides is very high. Also, with the location of Tabriz Airport in the vicinity of the fault, the occurrence of an earthquake can cause serious damage to it as well, which will lead to disruption of aid in the possible event of an earthquake. In the following, after obtaining seismic zoning for the study area, in order to evaluate the effect of soil stratification on seismic characteristics on the ground in terms of maximum acceleration and frequency content, in-well tests data from different parts of the range were collected in the area of city of Tabriz. As it is seen in Figure 7, an attempt has been made to examine the data used from all parts of the range resulting in appropriate distribution that is unique in terms of research records at the regional level.

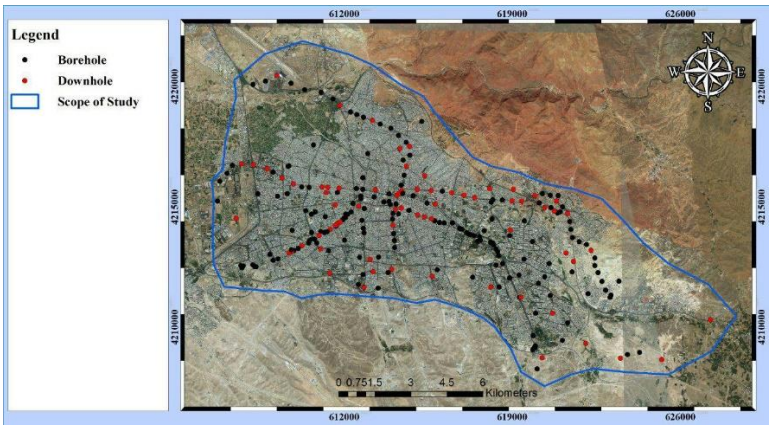

Figure 7. Scattering of collected data for evaluating amplification in study area.

Deepsoil software has been applied in order to obtain maximum seismic acceleration on the surface and magnify the effects of soil stratifications on it. Thus, having the seismic frequency in different parts of the range and using the collected geotechnical specifications, such as the thickness of the soil stratifications, particular weight, shear wave velocity and damping speed in different layers, all have been used as software input and the magnitude and effect of seismic frequency transmission from different soil stratifications in different samples have been obtained. By aggregating the results and displaying it in the study area, the seismic zoning after magnification applied to the surface in Arcmap software which is presented in Figure 8.

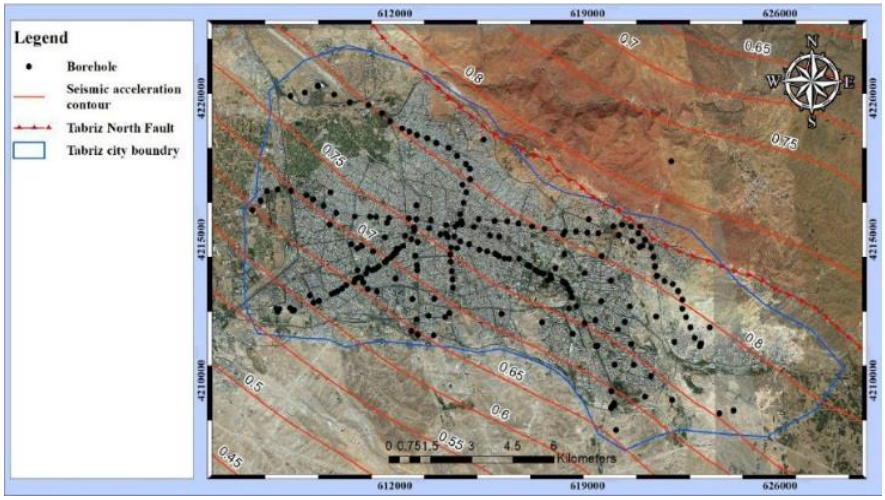

Figure 8. PGA values in study area based on amplification analysis.

5.2. Evaluation of Liquefaction Potential based on Standard Penetration Test Method (SPT)

Evaluation of the potential liquefaction of the soils in the study area was carried out based on the simplified method proposed by Idriss and Bolanger [2]. Then, safety factor (Fs) against liquefaction in soil layers is calculated. In continue, liquefaction potential index (LPI) was used for the assessment of the rate of liquefaction and the level of occurrence. One of the common methods is proposed by Iwasaki et al. [29, 30] introduced in the following equation:

$$LPI = \int_0^{20} W(Z) \times F(Z).dz \quad (10)$$

$$F(Z) = 1 - F_S \quad \text{For Fs} < 1 \quad (10a)$$

$$F(Z) = 0 \quad \text{For Fs} \geq 1 \quad (10b)$$

$$W(Z) = 10 - 0.5Z \quad \text{For Z} < 20 \text{ m} \quad (10c)$$

$$W(Z) = 0 \quad \text{For Z} > 20 \text{ m} \quad (10d)$$

Table 3: Liquefaction potential index (LPI) and its descriptions [29, 30].

LPI- Value	Liquefaction risk and investigation/ Countermeasures needed
LPI=0	Liquefaction risk is very low. Detailed investigation is not generally needed. (very low)
0<LPI≤ 5	Liquefaction risk is low. Further detailed investigation is needed especially for the important structures. (low)
5<LPI≤ 15	Liquefaction risk is high. Further detailed investigation is needed for structures. A countermeasure of liquefaction is generally needed. (high)
LPI> 15	Liquefaction risk is very high. Detailed investigation and countermeasures are needed. (very high)

Where, Z is the depth of midpoint in question layer. The Liquefaction intensity is stated between zeros and 100. The liquefaction risk can be obtained using Table 3 based on the liquefaction potential index (LPI) value.

5.3. Data Reliability Analysis (Data measurement)

According to Figure 9, each statistical study has different stages. The most important part is statistical analysis or statistical inference since this step acts as a control box that

determines and ensures accurate data collection, data calculation, and reliability of calculated data. It is significant since many obtained statistical data may lead to irrational and incorrect conclusion.

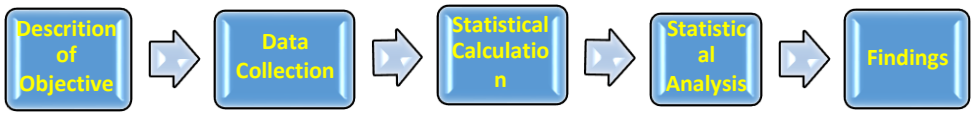

Figure 9. Data analysis process in terms of verification analysis.

Due to the nature of data collection, their classification can have human and computational errors. Therefore, it is required to monitor the data. In order to measure the data on the input data, determine the output results, and evaluate the potential of liquefaction in the soil layers based on the model introduced by Idriss and Bolanger [2], various statistical tests were carried out in EVIEWS 10 software, which are mentioned in the following:

5.3.1. Durability Test

A set of data is called a durable if its mean, variance, and covariance are independent of time (equal during the same interruptions). Mathematical variables inferred accurately from logical equations are durable; otherwise they must be turned durable.

$$E(x_t) = \mu \quad (11)$$

$$E[(x_t - \mu)^2] = Var(x_t) \quad (12)$$

$$E[(x_t - \mu)(x_{t-\mu} - \mu] = Cov(x_t, x_{t-\mu}) = \theta(\tau) \qquad t=1,2,3, \ldots \quad (13)$$

In the above equations, E (x_t) is the mathematical hope of the random variable X_t Due to probability of accidental process and false regression between variables, researchers examine the existence of a unit root in variables before estimation. It ensure that the variables are not fictitious followed by uncertain results so that it is required to certify that the variables are durable (not accidental). The unit root test is one of the most typical tests applied based on the Dickey-Fuller test to detect durability of process [31]. In this study, the statistical assumption test for each of the independent parameters (W.L, FC, $(N_1)_{60cs}$, TC, H, A) was carried out against the dependent parameter (LPI). In Table 4, as an instance of the result of the durable test, the groundwater level parameter, which is examined at levels 1%, 5% and

10% (the criterion is the level of 5%), reveals the durability of W.L. data. Table 5 also summarizes the results of the durability test for all independent modeled variables indicating the reliability of the data related to them. As it is observed, the probability result at all three levels is less than 0.0000, and the test result based on t-statistic distribution has absolute value greater than 2.

Table 4: Results of output for groundwater level factor (W.L) model based on Dickey- Fuller statistical test

Test critical values: (W.L)	**Level**	**t-Statistic**	**Prob**
Error Level	1%	-3.497727	0.0000
	5%	-2.890926	0.0000
	10%	-2.582514	0.0000
Augmented Dickey-Fuller test statistic		-5.809867	0.0000

Table 5: Results of the verification analysis of all the studied parameters in the present study based on the Dickey Fuller statistical test

Test Result	T Distribution	Significance Level	Variable
I(0)	-5.809867	0.0000 <	W.L
I(0)	-8.609178	0.0000 <	FC
I(0)	-8.043465	0.0000 <	$(N_1)_{60cs}$
I(0)	-7.802864	0.0000 <	TC
I(0)	-5.752662	0.0000 <	H
I(0)	-4.215421	0.0000 <	A
I(0)	-4.508944	0.0004	LPI

5.3.2. Autocorrelation Test (Breusch-Godfrey)

A classic assumption in regression is the lack of autocorrelation in statistical series [Cov (u_i, u_j) = 0]. Autocorrelation occurs in regression when the errors in the model are correlated. We apply this test if the regression has autocorrelation problem, or if a variable depends on the variables of the previous periods [32]. Table (6) summarizes the Breusch-Godfrey correlation test and, as it is seen from the results, the statistical values of F are higher than its significance level, so the H_0 assumption is acceptable and model is not auto correlated.

Table 6: Breusch-Godfrey's autocorrelation test on data variables affecting liquefaction

Breusch-Godfrey Serial Correlation Test	
F-Statistic	2.512839
Probability. F	0.0867
Prob. Chi-Square	0.0710

5.3.3. Heteroscedastic Test (White)

In estimating regression using the least squares method, first it is assumed that all error sentences have equal variances. When the model is estimated, it is examined applying a series of methods and techniques. A method in this regard is the White test. White test is typically used when the distribution of variance of the error sentences is not clear and there is no conjecture about it. Therefore, the White test assumes the most general state and is very sensitive to the diagnosis of heteroscedasticity [33]. The problem of heteroscedasticity concerns with the non-uniformity of variance and the dependent variable in different periods. It is assumed that as the independent variable increases or decreases, the variance of the dependent variable does not change. The cause of this problem can be related to the methods of collecting information or increase in the number of variables that cause errors in calculations. According to the results of the test statistics in Table 7, the values of the test statistics are higher than the values of its significant level, so the variance of the model is heteroscedastic. Therefore, in this model, a classic assumption, which is similar to variance, has been observed.

Table 7: Results of The white heteroscedasticity test variables affecting liquefaction.

White heteroscedasticity Test	
F-Statistic	1.981369
Probability. F	0.00881
Probability. Chi-Square	0.0321
Obs*R-Squared	1.992295

5.3.4. Collinearity Test (Correlation Matrix)

The latest statistical test carried out on the data is the collinearity test (correlation matrix) to analyze presence and absence of a linear relationship between the variables. Correlation matrix is a factor analysis that attempts to explain the changes in variables in more limited

factors or to determine the infrastructural features of a set of data. In this model, the data is converted into correlation matrices (covariance) and the correlation between each variable is obtained separately in matrix and a set of regression equations is developed between the variables that simply shows the correlation of some variables with each other. In the correlation matrix, the negative sign indicates the inverse relationship in the data, and these coefficients should be zero for equivalent variables and the direction of nonequivalent variables is numeric in the range [0.1]. The closeness of these coefficients to the number zero indicates lack of correlation, and the closer it is to the number one, the more the correlation between the two variables is [33]. Table 8 shows the correlation matrix between the variables effecting liquefaction.

Table 8: Matrix of correlations between effective variables in liquefaction

	LPI	W.L	A	TC	FC	$(N_1)_{60cs}$	H
LPI	1.000000	-0.416456	0.132198	0.586484	-0.230173	-0.562110	-0.263822
W.L	-0.416456	1.000000	-0.210037	-0.460157	-0.037844	0.023107	0.663566
A	0.132198	-0.210037	1.000000	0.028174	0.329111	0.335613	-0.080441
TC	0.586484	-0.460157	0.028174	1.000000	-0.222446	-0.172102	-0.154366
FC	-0.230173	-0.037844	0.329111	-0.222446	1.000000	0.299633	-0.101262
$(N_1)_{60cs}$	-0.562110	0.023107	0.335613	-0.172102	0.299633	1.000000	0.089297
H	-0.263822	0.663566	-0.080441	-0.154366	-0.101262	0.089297	1.000000

As it is observed, the highest linear relationship is between the variables of groundwater depth and liquefaction layer depth and the lowest linear relationship is between soil resistance coefficient and groundwater depth. Based on the analysis, it can be stated, concerning the statistical tests presented, the computational model of Idris and Bolanger (2010) has statistical coherence and necessity. Also, it is verified that all the data used to determine the liquefaction response of the soil area have a statistically consistent rhythm and the absence of data outside the range is confirmed. Therefore, with a probability of more than 95%, it is possible to acknowledge the results and indicate not making data in the calculations.

6. Results

The results of evaluation of the liquefaction potential in soil stratifications in the study area can be expressed as follows:

1- Of total 260 evaluated boreholes, 62 of them were determined with liquefaction potential. According to the study, concerning the results, a total of 61 layers of sandy soil and 11 layers of silt soil were assessed. The changes in the safety factor in the evaluated boreholes can be seen according to the fine percentage according to the Figure 10 below.

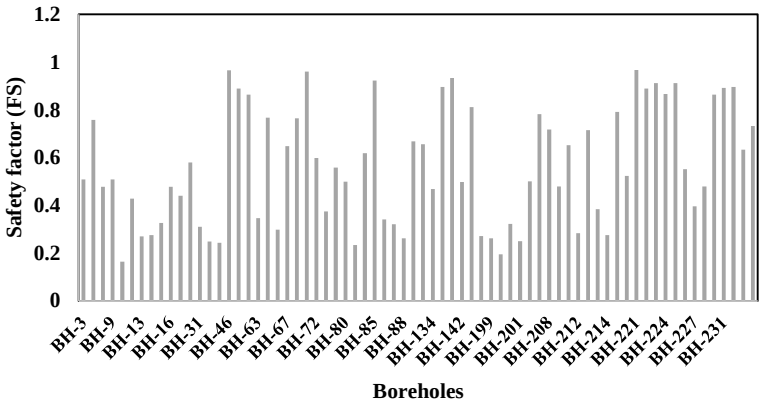

Figure10. Variation of safety factor in boreholes in study area

2- With the evaluation of 260 boreholes in the study area, the zoning map of Lubricity Risk Index (LPI) can be presented according to Figure 11. According to the results, the highest risk of liquefaction is limited to the southeastern regions of Tabriz. Also, a number of points with low liquefaction risk have been observed in the soil stratifications in the northeastern regions of Tabriz due to the type of materials and groundwater level.

3- The rate of changes in the Lubricity Risk Index of liquefaction in the city of Tabriz has been evaluated in the depth of soil stratifications in specified 5 axes in Figure 12. According to Figure 10 diagrams, the highest risk of liquefaction is observed in the lower soil stratifications on the I-J axis. Also, according to Figure 13 diagrams, lubricity risk in the soil stratifications in the eastern part of Tabriz is the lowest. However, according to the

liquefaction zoning curve, it can be seen that northeast of Tabriz has a minimum lubricity risk.

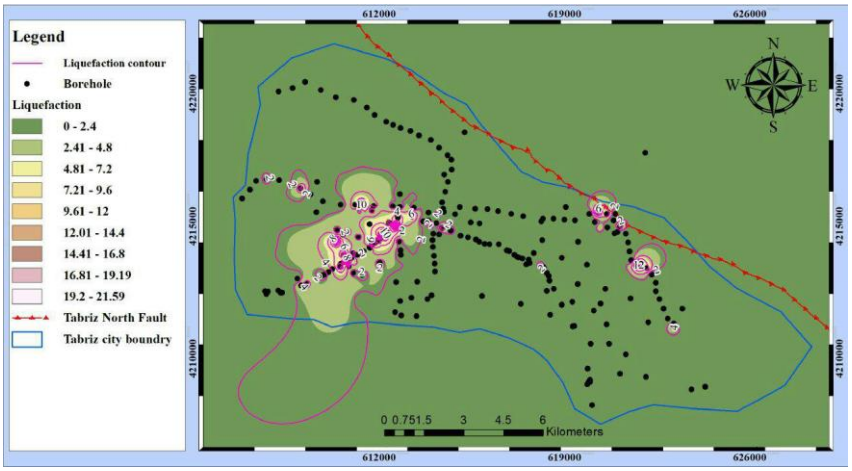

Figure11. Zoning map of liquefaction potential risks in study area.

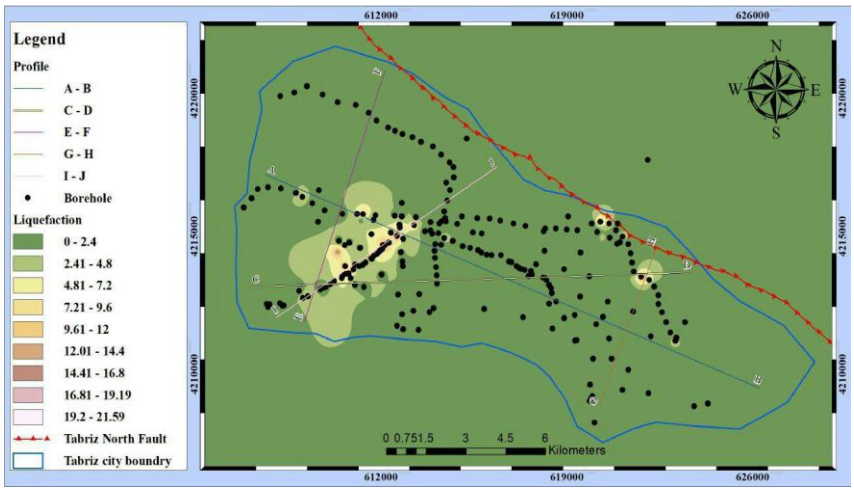

Figure 12. Location of five axes in study area for evaluation of LPI in soil layers.

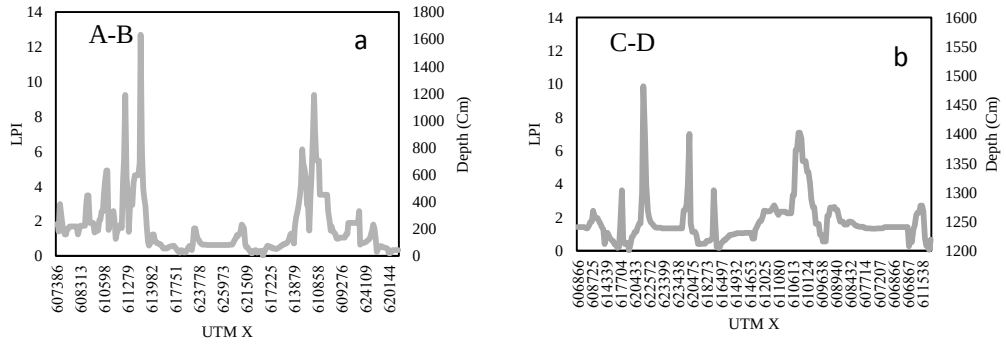

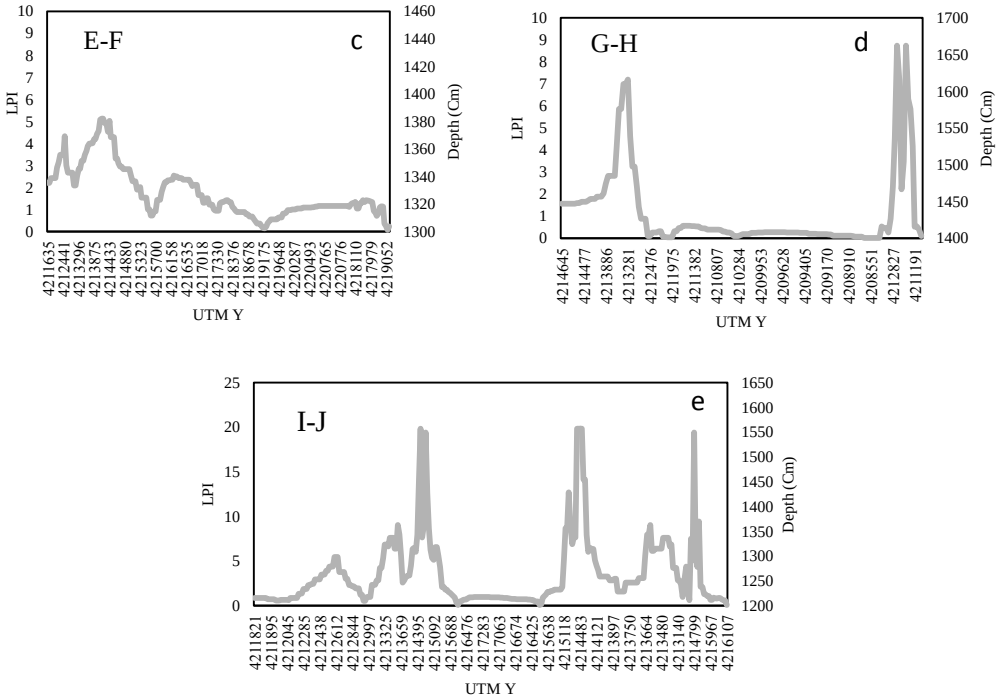

Figure 13. Variation of LPI in soil stratifications, a: A-B axes, b: C-D axes, c: E-F axes, d: G -H axes, e: I-J axes.

4- In the following, given that the effective parameters in determining the values of the dependent parameter is (y), which is (LPI), and independent parameters are Xi (WL, FC, TC, $(N_1)_{60cs}$, H, A), it was attempted to measure the effect of changes in independent variables on the dependent LPI variable. To this end, the sensitivity analysis method was applied using multi-layered perceptron neural network principles in MATLAB software. The multilayer perceptron, which is the most widely used neural network, has an input layer, an output layer, and a hidden layer or layers. In multilayer perceptron, the output of the first layer is the input vector of the second layer, and, similarly, the output of the second layer is the input vector of the third layer.

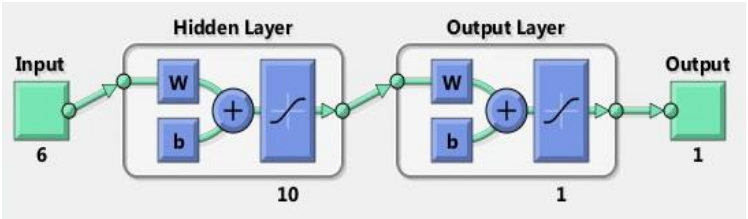

Figure14. The frame of neural network analysis used in the present study.

To this end, by deleting the data related to each of the effective parameters through combination of other independent variables in determining the dependent variable (LPI), the effect of that parameter was specified. Figure 15 presents an example of the results of this network in the P1 model scenario in which the impact of all independent parameters is involved, indicating a very logical and appropriate approach of the parameters in explaining the LPI values. Figure 16 shows the best validation performance and analysis history in neural network for P1 scenario. Also, based on Table 9, the effect analysis of parameters in different scenarios (P1, P2, .., P7) has been modeled and introduced. The coefficient of determination (R2) and the mean squared error (RMSE) are applied to determine and compare the accuracy of the models. These indicators are determined for each of the models of neural network and regression through the following equations:

$$R^2 = \frac{(\sum(x_i - \bar{x})(y_i - \bar{y}))^2}{\sum(x_i - \bar{x})^2 \sum(y_i - \bar{y})^2} \quad (14)$$

$$RMSE^2 = \frac{1}{n}\sum|x_i - y_i| \quad (15)$$

The transfer functions and the number of neurons in the hidden layer have been tested and the best network structure for each of the variables has been obtained. The best network selection is based on the lowest RMSE and the highest R^2 in MATLAB software. As it is observed from the results, the variable of groundwater depth (W.L) has the highest effect and the thickness of the liquefaction layer (TC) has the least effect among the effective parameters of sensitivity analysis.

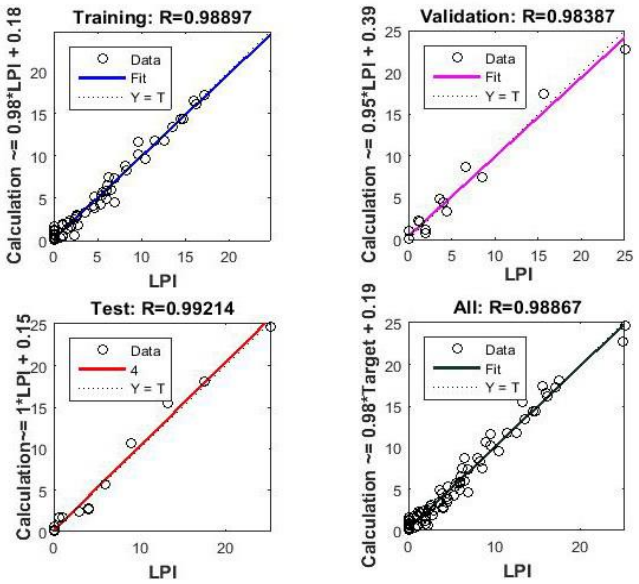

Figure 15. Model performance and LPI parameter analysis in ANN based on input parameters (W.L, FC, (N1) 60cs, TC, H, A) for P1 model scenario.

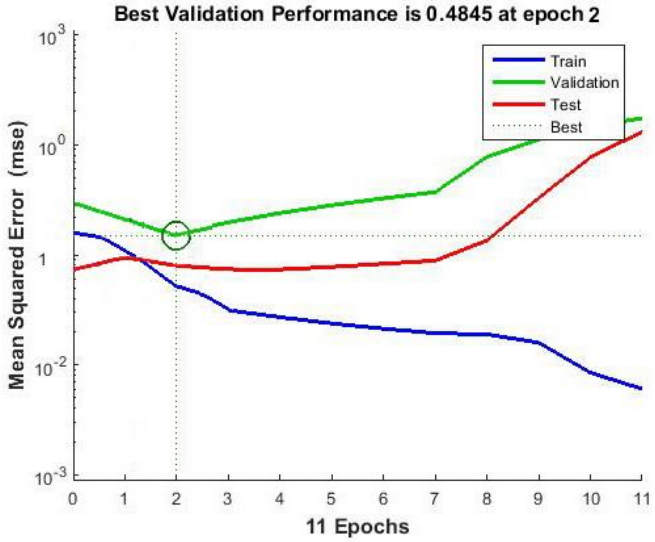

Figure16. The best ANN validation performance in P1 model sensitivity analysis.

Table 9: Comparison of sensitivity effects on LPI (dependent parameter) than independent parameters (A, H, TC, (N1) 60, FC, L, W.L).

	W.L	FC	$(N_1)_{60cs}$	TC	H	A(g)	R^2
P_1	✓	✓	✓	✓	✓	✓	0.97747
P_2	✓	✓	✓	✓	×	✓	0.80842
P_3	✓	✓	×	✓	✓	✓	0.82399
P_4	✓	×	✓	✓	✓	✓	0.89095
P_5	✓	✓	✓	×	✓	✓	0.93974
P_6	✓	✓	✓	✓	✓	×	0.90981
P_7	×	✓	✓	✓	✓	✓	0.67356

5- In order to estimate a probability model of liquefaction and an appropriate relation for evaluation of Lubricity Risk Index (LPI) in the study area, reliability analysis was carried out and Monte Carlo simulation model was applied according to Idris and Bolanger (2010) method. Also, parameters A, H, WL, FC, TC, $(N_1)_{60cs}$ according to Table 11 were considered as effective parameters in liquefaction.

Also, the set of random numbers of all boreholes with a safety factor of less than two (F.S≤2), which is a total of 74 boreholes, was measured. In addition, considering the confidence level (R = 80%) and the cumulative distribution limit (such as Z = 1.82) for calculations, the value of repetition (N) is considered to be about 1 million. By calculations and repetition of the direction of the data of the assumptions mentioned in MATLAB 2015 software, the graph of the probability density function against the safety factor was determined as Figure 17. It also turned out that the results did not change significantly after about 200,000 repetitions. The graph of the liquefaction probability was determined based on the safety factor at the error level of 5%, which is shown in Figure 18. Also, by calculating the changes in the liquefaction probability regarding safety factor (F.S), the graph of the changes is as following Figure 19.

Table.11: Evaluation of effective parameters on liquefaction based on Monte Carlo method.

Coefficient of variation (C.V)	Standard deviation (σ)	Average (μ)	Parameters
0.2580	3.5493	13.7560	H
0.4294	4.3495	10.1297	W.L
0.5175	15.4635	29.8783	FC
0.6484	3.0668	4.7297	TC
0.2454	6.2049	25.2793	$(N_1)_{60CS}$
0.0811	0.0585	0.7204	A

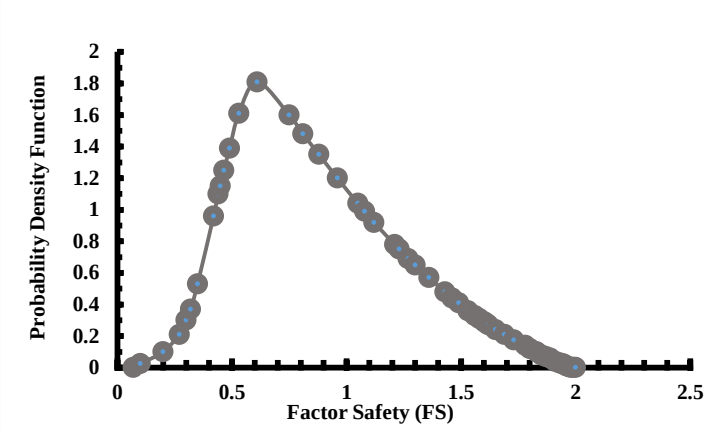

Figure17. Probability density function based on safety factor value in study area.

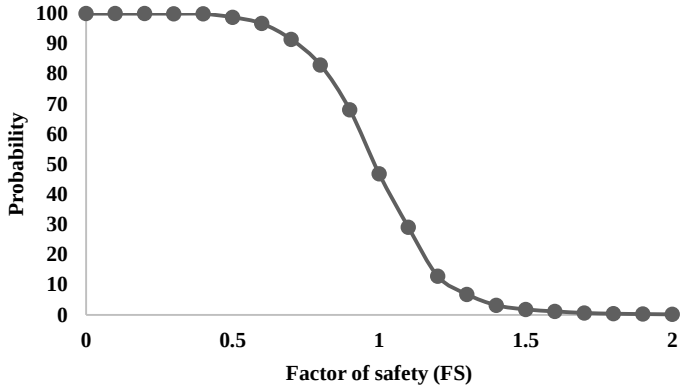

Figure18. Diagram of liquefaction probability based on safety factor in this study.

Based on Gauss-Newton's computational algorithm, relation (20) is introduced to describe this graph. This equation is obtained by 200 times with the tolerance of 0.00001.

$$PL = 1.3844 + (99.1796)\exp(-0.868004 \times F.S^{5.84638}) \quad (16)$$

By plotting the introduced equation alongside the Idriss and Bolanger (2014) [16] and Juang et al. (2012) [15] diagrams, the logical fitting and alignment of the above equation with the mentioned graphs are verified. In Figure 20, these samples are drawn together, indicating that the calculations have been confirmed.

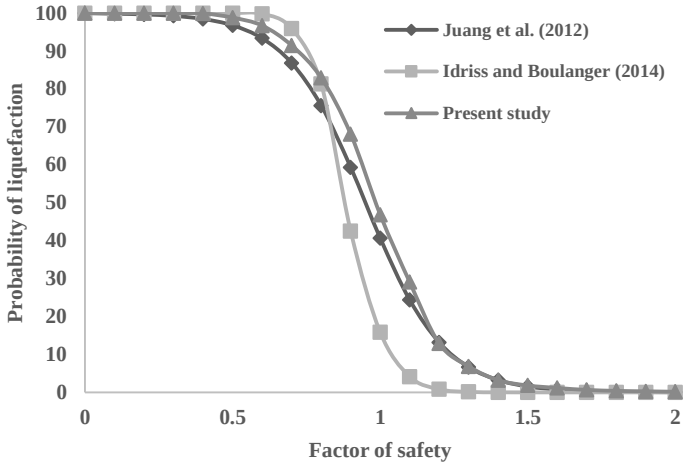

Figure 20. Comparison of diagram of liquefaction probability (in this study) with other methods based on safety factor parameter.

7. Conclusions

As noted in the previous sections, liquefaction is a main issue in seismic geotechnics. It occurs in earthquakes in granular soils with incomplete saturation. As a result, there is a decrease in volume between the soil particles that lead to extensive subsidence in the surface and subsurface soil stratifications, which can cause serious damage and destruction to geotechnical structures and buildings. In this study, it is attempted to evaluate the liquefaction potential in subsurface soil stratifications in the city of Tabriz through sensitivity analysis and reliability theory. The results of the present study can be stated as following:

A. Maximum surface acceleration, which is an important parameter in the occurrence of liquefaction, was evaluated, in the study area, by limited fault method using EXSIM program. Also, its expansion from bedrock to ground level was estimated by Deep soil v6.1 software. The results reveal that the maximum surface acceleration distribution near the fault is 0.8 g and in areas far from the fault is 0.4 g.

B. Of 260 boreholes evaluated, 62 of them with were identified liquefaction potential. According to the results of studies, the highest risk of liquefaction was observed in the southeastern part of Tabriz. The results obtained in studies by Ghasemian et al. [7] and Oshnoyeh and Dabiri [8] can be confirmed.

C- According to the sensitivity analysis on the data, it was observed that the groundwater level (W.L) and the depth of liquefaction stratification had the highest effect and the thickness

of the liquefaction stratification (TC) was the lowest among the effective parameters in the occurrence of liquefaction.

D. Finally, by calculating and plotting changes in the liquefaction probability against safety factor (FS), the equation of changes based on Gauss-Newton's computational algorithm (for the first time) was introduced, which is verified as it fits and aligns with diagrams plotted by Juang et al. [15], Idriss and Bolanger [16].

References

1. Seed, H. B., Idriss, I. M. & Arango, I. (1983). Evaluation of Liquefaction Potential Using Field Performance Data Journal of Geotechnical Engineering, ASCE, 109, 458-482.

2. Idriss, I. M., Boulanger, R. W. (2010). SPT-based liquefaction triggering procedures, Report no. UCD/CGM-10/02, Center for Geotechnical Modeling, University of California, Davis.

3. Noutash, K. M., Dabiri, R. & Hajialilue Bonab, M. (2012). Evaluating the liquefaction potential of soil in the south and southeast of Tehran based on shear wave velocity through empirical relationships Journal of Structural Engineering and Geotechnics, 2(1), 29-41.

4. Robertson, P. K., Wride, C. E. (1998). Evaluation Cyclic Liquefaction Potential Using the Cone Penetration Test, Canadian Geotechnical Journal, 35, 442-459.

5. Andrus, R. D., Stokoe, II. K. H. (2000). Liquefaction Resistance of Soils from Shear-Wave Velocity. Journal of Geotechnical and Geoenvironmental Engineering, ASCE, 126, 1015-1025.

6. Dabiri, R., Askari, F., Shafiee, A. & Jafari, M. K. (2011). Shear wave velocity based Liquefaction resistance of sand-silt mixtures: deterministic versus probabilistic approach, Iranian journal of science and technology, Transactions of civil engineering, 35, 199-215.

7. Ghasemian, M., Dabiri, R. & Mahari, R. (2018). Settlements hazards of soil due to liquefaction along Tabriz Metro Line 2, Pamukkale University Journal of Engineering Science, 24(6), 942-951.

8. Oshnaviyeh, D., Dabiri, R. (2018). Comparison of Comparison of Standard Penetration Test (SPT) and Shear Wave Velocity (Vs) Methods in Determining Liquefaction Hazard along Tabriz Metro Line 2, Journal of Engineering Geology, 12(2), 183-212. (In Persian)

9. Pourkermani, M., Mehraryan, M. (1997). Seismicity of Iran. Shahid Beheshti University, Iran.

10. Ansari, A., Noorzad, A. & Zafarani, H. (2008). Clustering analysis of the seismic catalog of Iran, Computers and Geosciences. Doi:0100105/j.cageo.11190100101.

11. Hamzehloo, H., Alikhanzadeh, A., Rahmani, M. & Ansari, A. (2012). Seismic Hazard Maps of Iran, The 4th World Conference on Earthquake Engineering, Lisbon.

12. Mojarab, M., Memarian, H., Zare, M., Hossein-Morshedy, A. & Pishahang, M. H. (2013). Modeling of the Seismotectonic Provinces of Iran using the Self-Organizing Map Algorithm, Computers and Geosciences, 59, 041–051.

13. Boore, D. M. (2009). Comparing stochastic point- and finite-source ground-motion simulations: SMSIM and EXSIM. Bulletin of Seismology Society of America, 99, 3202–3216.

14. Phoon, K. K., & F. H. Kulhawy. (2008). Reliability analysis of liquefaction potential of soils using standard penetration test. Chapter 13, Reliability-Based Design in Geotechnical Engineering: Computations and Applications, 497–526. Abingdon, UK: Taylor & Francis.

15. Juang, C. H., Ching, J., Luo, Z., & Ku, C. S. (2012), New models for probability of liquefaction using standard penetration tests based on an updated database of case histories. Engineering Geology, 133, 85-93.

16. Idriss, I., & Boulanger, R. W. (2014). CPT and SPT Based Liquefaction Triggering Procedures; Report UCD/CGM-14/01, Center for Geotechnical Modeling, Department of Civil and Environmental Engineering, University of California: Davis, CA, USA, April 2014; 77p.

17. Johari, A., Khodaparast, A. R. (2014). Analytical reliability assessment of liquefaction potential based on cone penetration test results, Journal of the Scientia Iranica, A, 21(5), 1549-1565.

18. Janalizade, A., Naghizaderokni, M. & Naghizaderokni, M. (2015). Reliability-based method for assessing liquefaction potential of soils, Proceedings, 5th ECCOMAS Thematic Conference on Computational Methods in Structural Dynamics and Earthquake Engineering, Crete Island, Greece, May 2015.

19. Pirhadi, N., Tang, X., Yang, Q., & Kang, F. (2019). A New Equation to Evaluate Liquefaction Triggering Using the Response Surface Method and Parametric Sensitivity Analysis, Journal of the Sustainability, 3, 20-35.

20. Zare, M. (2001). The risk of earthquakes and construction in the north of Tabriz fault zone and fault zone of earthquake faults in Iran. International Institute of Seismology and Earthquake Engineering. (In Persian)

21. Hartzell, S. (1978). Earthquake aftershocks as Green's functions. Geophysics Researches Letter, 5, 1–14.

22. Motazedian, D., Atkinson, G. (2005). Stochastic finite-fault model based on dynamic corner frequency. Bulletin of Seismology Society of America, 95, 995–1010.

23. Boore, D. M. (2003). Prediction of ground motion using the stochastic method. Pure Apply Geophysics, 160, 635–676.

24. Boore, D. M. (2005). SMSIM – Fortran programs for simulating ground motions from earthquakes: version 2.3, A revision of OFR 96-80-A, A modified version of OFR 00- 509. 59. [Online] Available from: (http://daveboore.com/software_online.html)

25. Samaei, M., Miyajima, M. & Yazdani, A. (2014). Prediction of Strong Ground Motion Using Stochastic Finite Fault Method: A Case Study of Niavaran Fault, Tehran, Geodynamics Research International Bulletin, 2(4), SN: 07.

26. Amiranlou, H., Pourkermani, M., Dabiri, R., Qoreshi, M. & Bouzari, S. (2016). The Stochastic Finite-Fault Modeling Based on a Dynamic Corner Frequency Simulating of Strong Ground Motion for Earthquake Scenario of North Tabriz Fault, Open Journal of Earthquake Research, 5, 114-121.

27. Ambraseys, N. N., Melville, CP. A. (1982). History of Persian Earthquakes, Cambridge University Press, UK.

28. Wells, D. L., Coppersmith, K. J. (1994). New empirical relationships among magnitude, rupture length, rupture width, rupture area, and surface displacement. Bulletin of Seismology Society of America, 84, 974–1002.

29. Iwasaki, T., Tokida, K., Tatsuko, F. & Yasuda, S. (1978). A practical method for assessing soil liquefaction potential based on case studies at various sites in Japan. Proceedings of 2nd International Conference on Microzonation, San Francisco, 885–896.

30. Iwasaki, T., Tokida, K., Tatsuoka, F., Watanabe, S., Yasuda, S., & Sato, H. (1982). Microzonation for soil liquefaction potential using simplified methods. Proceedings of 2nd International Conference on Microzonation, Seattle, USA, 1319–1330.

31. Dickey, A. & Fuller, W. A. (1979). Distribution of the Estimators for Autoregressive Time Series With a Unit Root, Journal of the American Statistical Association, 74(366), 427-431.

32. Godfrey, L. G. (1978). Testing for Higher Order Serial Correlation in Regression Equations When the Regressors Include Lagged Dependent Variables. Econometrica, 46, 1303-1310.

33. Aflatooni, A. (2017). Statistical analysis by Eviews. 3th Termeh Publication, Iran, 39-155.